THE JOURNAL OF BIOLOGICAL CHEMISTRY VOL. 290, NO. 19, pp. 12346–12354, May 8, 2015

The Wnt Signaling Antagonist Dapper1 Accelerates Dishevelled2 Degradation via Promoting Its Ubiquitination and Aggregate-induced Autophagy*

Received for publication, March 25, 2015, and revised form, March 30, 2015 Published, JBC Papers in Press, March 30, 2015, DOI 10.1074/jbc.M115.654590

Benyu Ma[1], **Bofeng Liu**[1], **Weipeng Cao, Chan Gao**[2], **Zhen Qi, Yuanheng Ning, and Ye-Guang Chen**[3]

From the State Key Laboratory of Biomembrane and Membrane Biotechnology, Tsinghua-Peking Center for Life Sciences, School of Life Sciences, Tsinghua University, Beijing 100084, China

Background: Protein aggregates could be degraded through autophagy.
Results: Dpr1 promotes pVHL-induced Dvl2 ubiquitination and mediates the Vps34-Beclin1 complex formation induced by protein aggregates.
Conclusion: Protein aggregates stimulate autophagy initiation in a Dpr1-dependent manner.
Significance: This study shows that protein aggregates can induce autophagy to facilitate their clearance.

Autophagy is a regulated process that sequesters and transports cytoplasmic materials such as protein aggregates via autophagosomes to lysosomes for degradation. Dapper1 (Dpr1), an interacting protein of Dishevelled (Dvl), antagonizes Wnt signaling by promoting Dishevelled degradation via lysosomes. However, the mechanism is unclear. Here, we show that Dpr1 promotes the von Hippel-Lindau tumor suppressor (VHL)-mediated ubiquitination of Dvl2 and its autophagic degradation. Knockdown of *Dpr1* decreases the interaction between Dvl2 and pVHL, resulting in reduced ubiquitination of Dvl2. Dpr1-mediated autophagic degradation of Dvl2 depends on Dvl2 aggregation. Moreover, the aggregate-prone proteins Dvl2, p62, and the huntingtin mutant Htt103Q promote autophagy in a Dpr1-dependent manner. These protein aggregates enhance the Beclin1-Vps34 interaction and Atg14L puncta formation, indicating that aggregated proteins stimulate autophagy initiation. Ubiquitination is not essential for the aggregate-induced autophagy initiation as inhibition of the ubiquitin-activation E1 enzyme activity did not block the aggregate-induced Atg14L puncta formation. Our findings suggest that Dpr1 promotes the ubiquitination of Dvl2 by pVHL and mediates the protein aggregate-elicited autophagy initiation.

Macroautophagy (hereafter referred to as autophagy) is a major intracellular degradation pathway in which aggregated proteins and damaged organelles are degraded, thereby contributing to maintaining the intracellular homeostasis and starvation responses (1–4). Autophagy is initiated by the formation of phagophore (also called isolation membrane) that requires phosphatidylinositol 3-phosphate generated by the Vps34 kinase complex (Beclin1, Vps34, Vps15, and the autophagy specific Atg14L). With engulfed cargos, the double-membrane of the phagophore extends and seals to form an autophagosome, which is eventually fused with lysosomes, leading to cargo degradation (5–7).

Because of misfolding or ubiquitination, the protein aggregates can be degraded by selective autophagy (termed aggrephagy) (8). In aggrephagy, the autophagy receptors, such as p62 and NBR1 that bind directly to LC3 and its homologs, interact with aggregated substrates and recruit them to autophagosomes (9, 10). ALFY, an Atg5-interacting autophagy receptor required for aggrephagy but not starvation-induced autophagy, can act as a scaffold protein to bridge polyglutamine (polyQ) aggregates to the Atg5-Atg12-Atg16 complex (11). In addition, it has been shown that Vps34, Atg14L, and Beclin1 can be recruited to certain ANK1-containing aggresomes (diameter >5 μm) (12), indicating that the Beclin1-Vps34-Atg14L complex may be involved in aggrephagy, but the detailed mechanism is still unknown.

Wnt signaling has essential functions in embryo development and tissue homeostasis, and its deregulation is associated with tumorigenesis and other diseases (13, 14). As a central mediator of Wnt signaling, Dishevelled (Dvl)[4] plays an important role in both β-catenin-mediated canonical and β-catenin-independent noncanonical Wnt signaling (14). We have shown that autophagy attenuates Wnt signaling by promoting Dvl2 degradation in mammalian cells (15). The von Hippel-Lindau tumor suppressor (pVHL), a component of the SCF-like ubiquitin E3 ligase complex, mediates Dvl2 ubiquitination, which in turn promotes Dvl aggregation and LC3/p62-mediated recruitment to autophagosomes for degradation under starvation.

Dapper1 (Dpr1/DACT1), originally identified as a Dvl-interacting protein (16), has been shown to mediate Dvl degradation

* This work was supported by National Natural Science Foundation of China Grant 31221064 and the 973 Program Grants 2010CB833706 and 2011CB943803 (to Y. G. C.).
[1] Both authors contributed equally to this work.
[2] Present address: Genomics Institute of the Novartis Foundation, 10675 John J. Hopkins Dr., San Diego, CA 92121.
[3] A Bayer-endowed Chair Professor. To whom correspondence should be addressed: Tel.: 86-10-62795184; Fax: 86-10-62794376; E-mail: ygchen@tsinghua.edu.cn.

[4] The abbreviations used are: Dvl, Dishevelled; 3-MA, 3-methyladenine; BFA1, bafilomycin A1; DFCP1, double FYVE-containing protein 1; Dpr1, Dapper1; HBSS, Hanks' balanced salt solution; Htt103Q, huntingtin fragment carrying an expanded polyglutamine; MEF, mouse embryonic fibroblast; NRK cell, normal rat kidney cell; Hsp, heat shock protein; VHL, von Hippel-Lindau tumor suppressor.

and thus inhibit both Dvl-mediated canonical and noncanonical Wnt signaling (17–19). Recently, we found that Dpr1 can promote autophagy initiation by enhancing the Vps34-Beclin1-Atg14L complex formation, and loss of Dpr1 in the central nervous system results in motor coordination deficiency and accumulation of ubiquitinated proteins (20). However, it is unclear how Dpr1 accelerates Dvl2 degradation. In this study, we report that Dpr1 enhances the interaction between Dvl2 and pVHL, thereby promoting the Dvl2 ubiquitination. Moreover, we observed that aggregated proteins could induce autophagy to accelerate their degradation, and Dpr1 promoted this process.

EXPERIMENTAL PROCEDURES

Cell Culture—HEK293T, NRK, NRK GFP-DFCP, and NRK CFP-LC3 stable cell lines were cultured in DMEM containing 10% fetal bovine serum (Hyclone) supplemented with 4 mM L-glutamine in 5% CO_2 at 37 °C, and the transfection was conducted with Vigofect (Vigorous Biotechnology, Beijing, China) according to the manufacturer's recommendations. Primary mouse embryonic fibroblast (MEFs) were generated from 13.5 day embryos from *Dpr1*$^{-/-}$ mattings (18) and were maintained in DMEM with 10% FBS added. For starvation, cells were first washed three times with PBS and cultured in Hanks' balanced salt solution (Invitrogen) for the indicated time.

Plasmid Construction—The pCMV-Myc/hDpr1 and pEGFP-C1/hDpr1 plasmids have been described previously (17). The hVps34 cDNA was cloned from pCS2/Vps34 into the KpnI and XbaI sites of pCS2(+)-FLAG. The HA-Beclin1 vector was a kind gift from Honggang Wang. Dvl2 was cloned into the BamHI site of pDsRed-N1 (Invitrogen) and pCS2(+)-FLAG. The CFP-LC3 was a gift from Dr. Li Yu. The Atg14L was cloned from GFP-Atg14L (a gift from Dr. Li Yu) into the EcoRI and ClaI sites of pcDNA3.1(+)-FLAG. pCDNA3.1/HA-Dvl2(WT), pCDNA3.1/HA-Dvl2(M1), and pCDNA3.1/HA-Dvl2(M2) were described previously (15). FLAG-Vps15 was cloned into HindIII and ClaI sites of pcDNA3.1-FLAG. GFP-Atg16L was a gift from Dr. Hong Zhang. Hsp70 and Hsp90 were gifts from Dr. Zhijie Chang. *Dpr1* and *VHL* shRNAs were purchased from Open Biosystems. The sequence of *VHL* siRNA is as follows: 5′-GAGGUCACCUUUGGCUCUUTT-3′ (GenePharma). VHL shRNA was purchased from Open Biosystems.

Antibodies and Reagents—3-Methyladenine (3-MA) was obtained from Sigma and prepared in distilled water. MG132 (Calbiochem) was prepared in DMSO. Bafilomycin A1 (BFA1) was purchased from Sigma and prepared in DMSO. Antibodies include the following: mouse anti-Beclin1 (BD Biosciences); rabbit anti-Beclin1 (MBL); rabbit anti-Vps34 (Cell Signaling); rabbit anti-Atg14L (MBL); mouse anti-FLAG M2 (Sigma); rabbit anti-Dvl2 (Cell Signaling); mouse anti-tubulin and anti-GFP (Santa Cruz Biotechnology); mouse anti-p62 and anti-pVHL (BD Biosciences); and rabbit anti-LC3 (MBL).

Immunoblotting and Immunoprecipitation—For immunoblotting, cells were lysed at 4 °C for 15 min in lysis buffer (20 mM Tris-HCl, pH 7.4, 150 mM NaCl, 2 mM EDTA, 25 mM NaF, 1% Triton X-100) plus complete protease inhibitor mixture (Roche Applied Science). After 12,000 rpm centrifugation for 15 min at 4 °C, the supernatants were resolved by SDS-PAGE and transferred to NC membranes. The membranes were blocked with TBST containing 5% nonfat dry milk and incubated overnight at 4 °C with primary antibodies. Membranes were washed with TBST three times, incubated for 1 h at room temperature with HRP-conjugated secondary antibodies (Amersham Biosciences), and then washed. Immunoreactive bands were visualized by chemiluminescence (ECL Plus from Thermo Scientific).

For immunoprecipitation, cells were lysed with lysis buffer containing complete protease inhibitor mixture (Roche Applied Science) for 30 min at 4 °C. Lysates were cleared by centrifugation at 12,000 rpm for 15 min at 4 °C. The supernatants were immunoprecipitated with specific antibodies and protein A-Sepharose (Zymed Laboratories Inc.). Immunocomplexes were washed three times with washing buffer (50 mM Tris-HCl, pH 8.0, 150 mM NaCl, 1% Nonidet P-40, 0.5% sodium deoxycholate) and analyzed by immunoblotting.

Adenoviral Expression—HA-Dvl2 was subcloned into the KpnI and XhoI sites of pShuttle-CMV vector (Invitrogen) and transferred into pAdEasy-1 vector (Invitrogen) by performing the Clonase LR recombination reaction (Invitrogen). The production of adenovirus and adenovirus infection was performed according to the manufacturer's protocols.

Immunofluorescence Microscopy—Immunofluorescence analysis was performed as described previously (15). Cells grown on glass coverslips in six-well plates were transfected with the indicated plasmids for 24 h. After washed twice with PBS, the cells were fixed with 4% paraformaldehyde for 20 min at room temperature, permeabilized for 10 min with 0.2% Triton X-100 (Sigma), and blocked with 5% BSA in PBST (phosphate-buffered saline plus Tween 20) for 1 h. Before subjecting to secondary antibodies (Jackson ImmunoResearch) for 1 h at room temperature, the cells were incubated with the primary antibodies overnight at 4 °C and washed with PBST three times. Confocal laser scanning of fixed cells was detected using a Zeiss LSM 710 laser scanning microscope.

Quantitation of Protein Puncta—The number of CFP-LC3 and Atg14L-mCherry puncta was measured by Image-ProPlus software. CFP-LC3 and Atg14L-mCherry puncta were quantified from at least 20 different cells in three separate experiments. These measurements were done on randomly selected fields of view. In addition, all data reported that show differences in puncta formation were verified qualitatively in blind fashion by an independent observer.

Statistical Analysis—Statistical analyses were performed using a two-tailed unpaired *t* test. *p* values of <0.05 were considered statistically significant. *n* represents the number of independent experiments used for statistical analysis.

RESULTS

Dpr1 Facilitates Dvl2 Degradation via Autophagy—We have previously shown that Dpr1 could promote Dvl2 degradation in a lysosomal inhibitor-sensitive manner (19), and Dvl could be degraded via autophagy (15). To test whether Dvl degradation induced by Dpr1 is dependent on autophagy, we examined the effect of the class III phosphatidylinositol 3-kinase inhibitor 3-methyladenine (3-MA), which is commonly used to block autophagy (21, 22), on the Dpr1-mediated Dvl turnover. As shown in Fig. 1*A*, co-expression of Dpr1 accelerated Dvl2 deg-

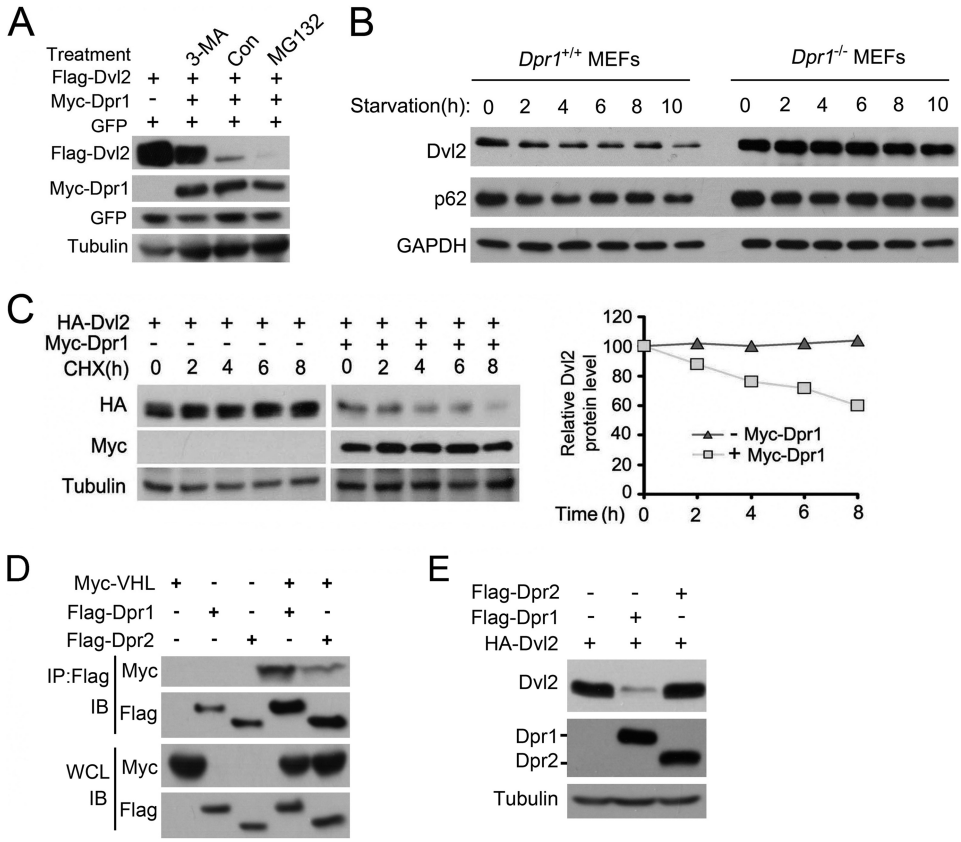

FIGURE 1. **Dpr1 facilitates Dvl2 degradation via autophagy.** *A,* Dpr1-mediated Dvl2 degradation was rescued by 3-MA (5 mM) but not by MG132 (1 μM). HEK293T cells transfected with the indicated plasmids were treated with the indicated inhibitors for 6 h before being harvested for immunoblotting. GFP was used as a transfection control (*Con*). *B,* half-life of Dvl2 was prolonged in *Dpr1*$^{-/-}$ MEFs. Wild-type or *Dpr1*$^{-/-}$ MEFs were cultured in Hanks' balanced salt solution medium (starvation) for the indicated times before being harvested for immunoblotting with the indicated antibodies. p62 was detected as a autophagy marker. *C,* Dpr1 accelerated Dvl2 degradation in HEK293T cells. The cells transfected with the indicated plasmids were treated with the translation inhibitor cycloheximide (10 μM) for various times before being harvested for immunoblotting. The relative band intensity of Dvl2 was quantified and is shown at the *right*. *D,* pVHL interacted with Dpr1 and its homolog Dpr2. HEK293T cells were transfected with the indicated constructs and harvested for anti-FLAG immunoprecipitation (*IP*) and then anti-Myc immunoblotting (*IB*). *E,* Dpr1 but not Dpr2 promoted Dvl2 degradation.

radation, and this process was attenuated by 3-MA, but not by the proteasome inhibitor MG132, suggesting that Dpr1 induced Dvl2 degradation via the autophagy pathway. As a control, the GFP expression level was not affected by Dpr1, indicating that the reduced Dvl2 level was not due to the expression competition between proteins. The starvation-induced Dvl2 turnover was attenuated by *Dpr1* knock-out, consistent with reduced autophagic flux shown by p62 in *Dpr1*$^{-/-}$ cells (Fig. 1*B*). Furthermore, overexpression of Dpr1 dramatically increased the degradation rate of Dvl2 (Fig. 1*C*). In contrast, Dpr2, a homolog of Dpr1, could also interact with Dvl2 (Fig. 1*D*), but it had no effect on Dvl2 stability (Fig. 1*E*). Together, these data indicate that Dpr1 facilitates Dvl2 degradation via autophagy.

Dpr1 Promotes the pVHL-mediated Dvl2 Ubiquitination—Our previous data indicate that Dvl2 ubiquitination is critical for its autophagy-mediated degradation (15). Then we tested whether Dpr1 affected Dvl2 ubiquitination. As shown in Fig. 2*A*, Dpr1 dramatically increased Dvl2 ubiquitination. In agreement with our previous report (15), when the cells were treated with the lysosomal inhibitor bafilomycin A1 (BFA1), nutrient starvation caused increased Dvl2 ubiquitination, and Dpr1 could further enhance the level (Fig. 2*A*). The promoting effect of Dpr1 on Dvl2 ubiquitination was confirmed by knockdown of *Dpr1* under both starvation and normal conditions (Fig. 2*B*). As pVHL, a component of the SCF-like ubiquitin E3 ligase complex, can induce Dvl2 ubiquitination (15), we examined whether Dpr1-enhanced Dvl2 ubiquitination is mediated by pVHL. Knockdown of *VHL* decreased the ubiquitinated Dvl2 level (Fig. 2*C*). Furthermore, *VHL* depletion rescued the Dpr1-induced Dvl2 degradation (Fig. 2*D*). These data together indicate that Dpr1-induced ubiquitination and degradation of Dvl2 depend on pVHL.

As Dpr1 interacts with Dvl proteins, it may function as a scaffold to strengthen the association between Dvl2 and pVHL. To test this possibility, we first examined whether Dpr1 could interact with pVHL. As shown in Fig. 2*E*, pVHL was found in the Dpr1 immunoprecipitant, indicating that these two proteins interact with each other. pVHL contains two major domains as follows: the α domain (153–204 amino acids) that binds to the elongin/Cullin2/Rbx1, and the β domain (63–152 amino acids) that binds directly to the substrates such as HIFα (23). We found that pVHL interacted with Dpr1 via its α domain (Fig. 2*E*). Domain mapping also revealed that the N terminus of Dpr1 was needed to interact with pVHL (Fig. 2*F*), which is different for Dpr1 interaction with Dvl2 via its C terminus (19). To further confirm the scaffold function of Dpr1, we knocked down *Dpr1* expression and found that reduction of

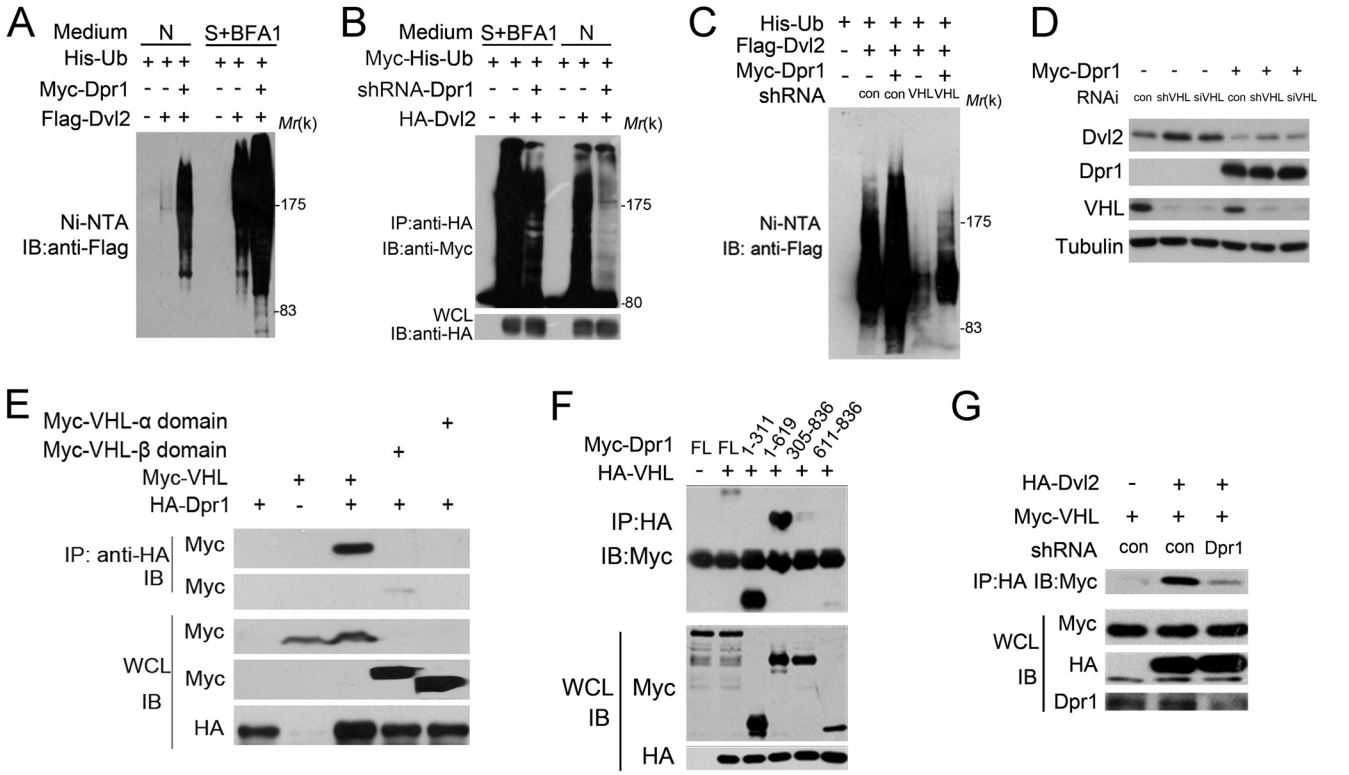

FIGURE 2. **Dpr1 promotes pVHL-mediated Dvl2 ubiquitination.** *A,* Dvl2 ubiquitination (*Ub*) was enhanced by Dpr1 overexpression under both nutrient-rich (*N*) and starvation (*S*) conditions. HEK293T cells transfected with the indicated constructs were treated with 100 nM BFA1 for 6 h. Ubiquitinated proteins were precipitated with nickel-nitrilotriacetate (*Ni-NTA*) beads, followed by anti-FLAG immunoblotting. *B, Dpr1* knockdown decreased Dvl2 ubiquitination under both starvation (*S*) and nutrient-rich (*N*) conditions. HEK293T cells transfected with indicated constructs were treated with 100 nM BFA1 for 6 h. Ubiquitinated proteins were precipitated with anti-HA antibody, followed by anti-Myc immunoblotting (*IB*). The cell lysates were adjusted to equal Dvl2 protein levels to have a fair comparison with the Dvl2 ubiquitination levels. *C,* Dvl2 ubiquitination elevated by Dpr1 was decreased by *VHL* knockdown. *D,* Dpr1-promoted Dvl2 degradation was attenuated by *VHL* knockdown under starvation condition. *E,* pVHL interacted with Dpr1 via its α domain. HEK293T cells transfected with the indicated constructs were harvested for immunoprecipitation (*IP*) by anti-HA antibody, followed by anti-Myc immunoblotting. *F,* Dpr1 interacted with pVHL through its N terminus. *G, Dpr1* knockdown reduced the pVHL-Dvl2 interaction.

Dpr1 decreased the interaction between the Dvl2 and pVHL (Fig. 2*G*). These data indicate that Dpr1 facilitates the interaction between Dvl2 and pVHL, therefore promoting Dvl2 ubiquitination.

Dpr1 Mediates Dvl2 Aggregate-induced Autophagy—Our previous work has shown that Dpr1 induces Dvl2 degradation through the lysosome (19), and Dvl2 aggregates could be degraded by the autophagy-lysosome pathway (Fig. 1). Dvl proteins undergo aggregation in the cytoplasm through its DIX domain (24, 25), and the aggregation-deficient mutants of Dvl2 are resistant to the autophagy-mediated degradation (15). Therefore, to access whether Dpr1-mediated Dvl2 degradation is dependent on its aggregation, we examined the protein levels of wild-type Dvl2 and aggregation-deficient mutants upon Dpr1 expression. Although Dpr1 overexpression accelerated the degradation of wild-type Dvl2, it had minimal effect on Dvl2 mutants M1 (F43S) and M2 (V67A/K68A) (Fig. 3*A*), indicating that Dvl2 aggregation is required for its Dpr1-induced clearance. Then we tested whether the aggregation of Dvl2 could stimulate the autophagy, and we found that Dvl2 overexpression could increase the puncta formation of LC3 in NRK cells (Fig. 3*B*). Furthermore, Dvl2 overexpression reduced p62 protein level in *Dpr1*$^{+/+}$ but not in *Dpr1*$^{-/-}$ MEFs (Fig. 3*C*), indicating that Dvl2 could induce the autophagy dependent on Dpr1.

Previously we have reported that Dpr1 induces the autophagy initiation through promoting the Beclin1-Vps34-Atg14L complex formation (20), so we investigated whether Dvl aggregates could stimulate autophagy via the Beclin1-Vps34-Atg14L-Dpr1 complex under nutrient-rich conditions. Indeed, wild-type Dvl2, but not the M1 mutant, induced Atg14L puncta formation in NRK cells (Fig. 3*D*) and further increased the Dpr1-induced DFCP1 puncta formation (Fig. 3*E*). Consistently, wild-type Dvl2 enhanced the Beclin1-Vps34 complex formation, although both Dvl2 mutants M1 and M2 had no enhancement on this interaction (Fig. 3*F*). Wild-type Dvl2 could further increase the Vps34-Beclin1 interaction induced by Dpr1 (Fig. 3*G*). Taken together, these data indicate that Dvl2 aggregates facilitate Dpr1-induced autophagy.

Dpr1 Has a More General Role on Protein Aggregate-induced Autophagy—Similar to Dvl aggregates, some other aggregate-prone proteins, such as p62 and Htt103Q (huntingtin fragment carrying an expanded polyglutamine), have been shown to undergo autophagy-mediated degradation (15, 26, 27). We thus assessed whether these aggregates promote autophagy under nutrient-rich conditions. Overexpression of p62-GFP or Htt103Q-GFP increased the number of the Atg14L-mCherry dots (Fig. 4*A*), whereas the p62 D69A mutant, which is aggregation-deficient (28), failed to do so (Fig. 4*B*). Similarly, ectopically expressed Htt103Q and wild-type p62, but not p62 D69A

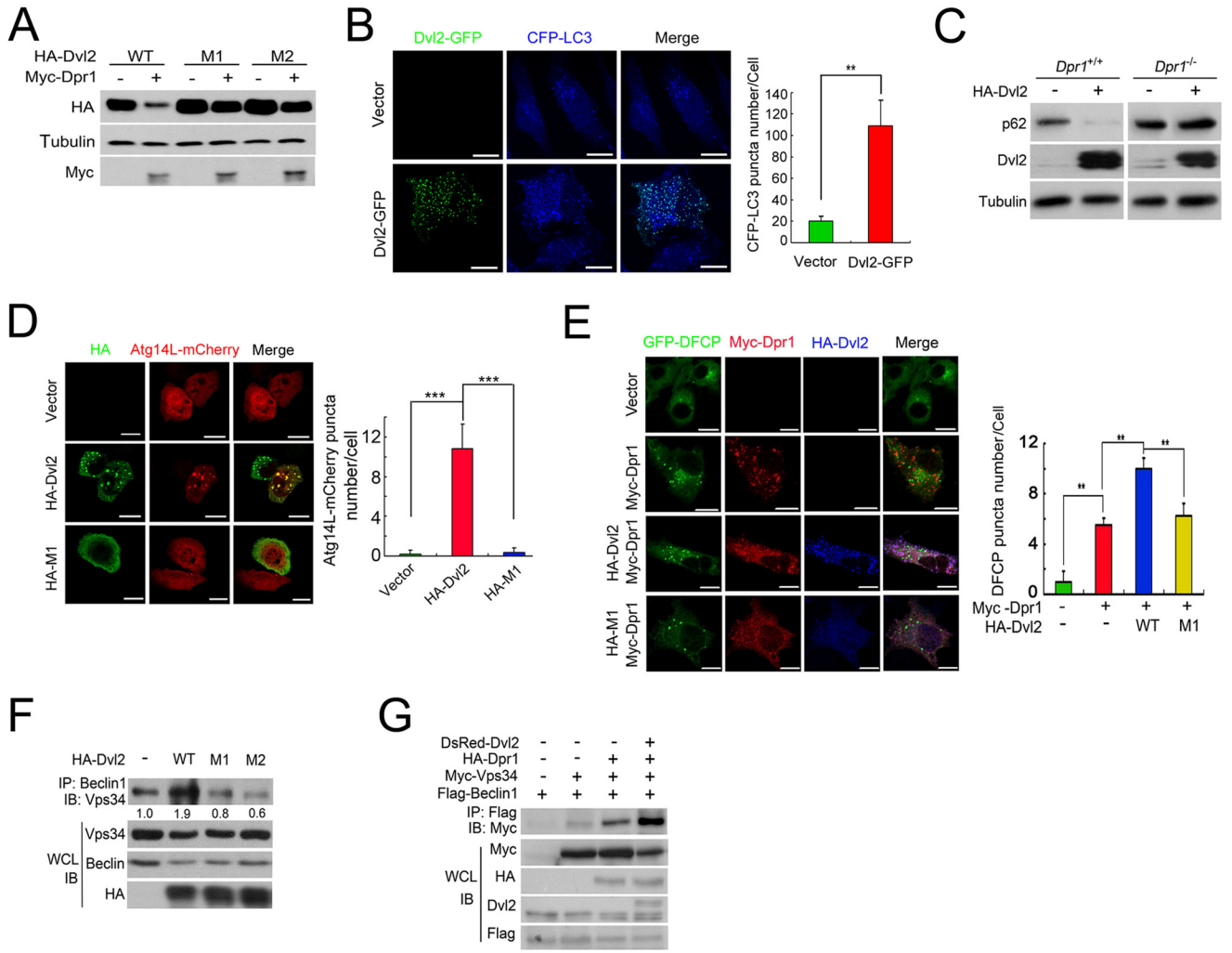

FIGURE 3. **Dvl2 stimulates autophagy initiation, which is dependent on its aggregation.** *A,* Dpr1-enhanced degradation of wild-type Dvl2, but not its aggregation-deficient mutants. HEK293T cells transfected with the indicated constructs were harvested for immunoblotting with the indicated antibodies. *B,* wild-type Dvl2 induced the LC3 puncta formation in NRK cells. NRK cells transfected with the indicated plasmids were fixed with 4% paraformaldehyde for immunofluorescence. The puncta number per cell was quantified ($n = 3$). *Scale bars,* 10 μm. **, $p < 0.01$. Data were represented as mean ± S.D. *C,* Dvl2 promoted p62 degradation in a Dpr1-dependent manner. Immunoblotting is shown of p62 levels in $Dpr1^{+/+}$ and $Dpr1^{-/-}$ MEFs infected with or without Dvl2-expressing adenovirus. *D,* wild-type Dvl2, but not its M1 mutant, facilitated the Atg14L-mCherry puncta formation. The puncta number per cell was quantified ($n = 3$). *Scale bars,* 10 μm. ***, $p < 0.001$. Data were represented as mean ± S.D. *E,* wild-type Dvl2, but not its M1 mutant, enhanced the Dpr1-mediated GFP-DFCP1 puncta formation. The puncta number per cell was quantified ($n = 3$). *Scale bars,* 10 μm. **, $p < 0.01$. Data were represented as mean ± S.D. *F,* ectopic expression of wild-type Dvl2, but not M1 and M2 mutants, enhanced the Beclin1-Vps34 interaction. *IP*, immunoprecipitation; *IB*, immunoblot; WCL, whole cell lysate. *G,* Dvl2 further increased the Dpr1-promoted Beclin1-Vps34 interaction in HEK293T cells.

mutant, led to LC3 puncta formation (Fig. 4*C*). These Atg14L-mCherry and CFP-LC3 dots were well co-localized with p62-GFP or Htt103Q-GFP under nutrient-rich conditions. These data clearly support the notion that protein aggregates can induce autophagy. Moreover, p62 increased Atg14L-mCherry dot formation in wild-type MEFs under nutrient-rich conditions, but this function was dramatically reduced by *Dpr1* deletion (Fig. 4*D*), indicating that Dpr1 is critical for p62-induced autophagy initiation.

Although overexpression of p62 and Htt103Q did not influence the activity of AMP-activated protein kinase and mammalian target of rapamycin by examining the phosphorylation levels of their respective substrates ULK1 and S6K (Fig. 5*A*), they efficiently enhanced the interaction between Vps34 and Beclin1 (Fig. 5*B*), which was reduced by *Dpr1* depletion (Fig. 5*C*). Dpr1 overexpression also accelerated the turnover of p62 and Htt103Q (Fig. 5, *D*–*G*). These data together suggest that protein aggregates can induce autophagy by increasing the Beclin1-Vps34 interaction, and this induction is dependent on Dpr1.

Ubiquitination Is Not Essential for the Aggregate-induced Autophagy Initiation—To explore the mechanism underlying the aggregate-inducted autophagy initiation, we tested whether the autophagy initiation effectors could preferentially recognize the aggregates but not their nonaggregates mutants. As shown in Fig. 6*A*, Atg14L bound to wild-type Dvl2 and the Dvl2 M1 mutant equally. Similarly, Vps15, a common regulator of the Vps34 complex, interacted with Dvl2 wild-type and the M1 mutant with a similar affinity (Fig. 6*B*). Interestingly, overexpression of Dvl2 and p62 induced Vps15 from a diffusing distribution to a puncta formation (Fig. 6*C*), consistent with protein aggregate-induced autophagy initiation. Because the

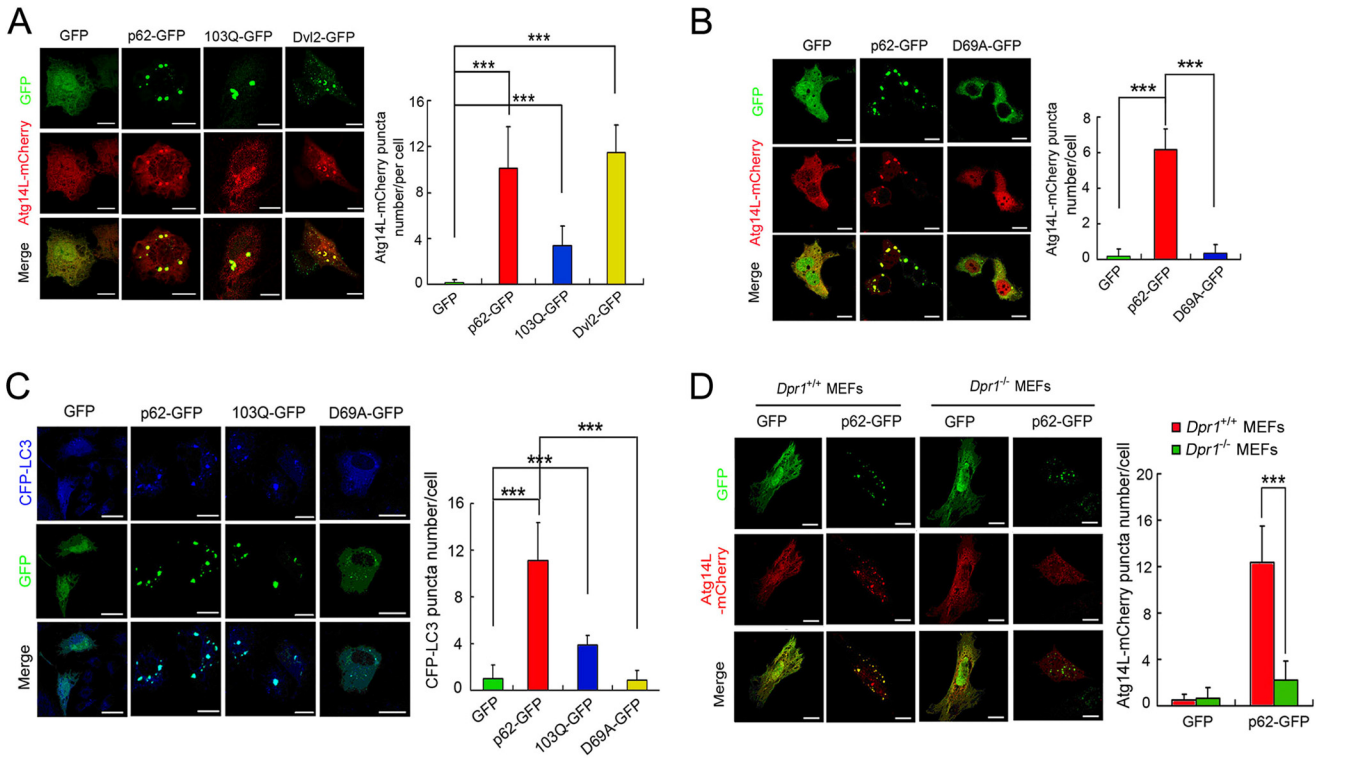

FIGURE 4. **Dpr1 plays a general role in protein aggregates initiating autophagy.** *A,* p62-GFP, Htt103Q-GFP, and Dvl2-GFP promoted the Atg14L-mCherry puncta formation in NRK cells. *B,* wild-type p62, but not its D69A mutant, promoted the Atg14L-mCherry puncta formation in HEK293T cells. *C,* wild-type p62 and Htt103Q, but not p62 D69A mutant, enhanced CFP-LC3 puncta formation in CFP-LC3-stable NRK cells. *D,* p62-induced Atg14L-mCherry puncta formation was attenuated in *Dpr1*$^{-/-}$ MEFs. The puncta number per cell was quantified ($n = 3$). *Scale bars,* 10 μm. ***, $p < 0.001$. Data were represented as mean ± S.D.

WD40 domain of Vps15 could recognize and bind to ubiquitin (29), we tested whether this domain is important for the aggregate-induced autophagy initiation, and we found that deletion of the WD40 domain had no effect on the puncta formation of Vps15 upon Dvl2 or p62 overexpression (Fig. 6*C*). Atg16L, another WD40 domain-containing protein, is required for the recognition of ubiquitinated endosomes upon *Salmonella* infection (30). Surprisingly, we observed a strong interaction between Dvl2 M1 and M2 mutants and Atg16L, which is important for LC3-phosphatidylethanolamine conjugation, compared with wild-type Dvl2 (Fig. 6*D*). However, no association was observed between Atg16L with either wild-type p62 or its D69A mutant. Taken together, these data indicate that none of the Vps15, Atg14L, and Atg16L preferentially recognizes the aggregates over their aggregation-deficient mutants.

Misfolded protein aggregates can be recognized by heat shock proteins (Hsp), which can help with refolding or mediating degradation of the aggregates through the proteasome pathway (31). It was recently reported that acetylated Hsp70 is required for the Beclin1-Vps34 complex formation and autophagosome formation (32). Therefore, we examined whether Hsp70 is involved in the autophagy formation stimulated by Dvl2 and p62 aggregates. However, we found that Dvl2 and p62 aggregates could not induce the puncta formation of Hsp70 (Fig. 6*E*). Similar results were observed with Hsp90. These data suggest that Hsp70 and Hsp90 are not involved in the aggregate-induced autophagy initiation.

Ubiquitination and aggregation have been shown to have a mutually promoting effect, and ubiquitination plays an important role in protein aggregate degradation via autophagy (33, 34). Ubiquitination also plays a vital role in the recruitment of the autophagic machinery to endosomes during *Salmonella* infection (30). Therefore, we wanted to explore whether ubiquitination is critical for the aggregate-induced autophagy. To this end, we examined whether p62 aggregates are co-localized with endogenous ubiquitin. As shown in Fig. 6*F*, p62 aggregates were nicely co-localized with LC3, consistent with the stimulatory effect of p62 aggregates in autophagosome formation. Although most of the p62-LC3 co-staining puncta were co-localized with endogenous ubiquitin, some of them were not. Similarly, some LC3 puncta induced by Dvl2 aggregates were not co-localized with endogenous ubiquitin (Fig. 6*G*). Taken together, these data indicate that ubiquitin is not essential for LC3 puncta formation induced by protein aggregates.

To further address the function of ubiquitin in aggregate-induced autophagy, we employed the ubiquitin-activation E1 enzyme inhibitor PYR-41 to block the ubiquitin-conjugation process (35). Although the ubiquitin-conjugation process was efficiently blocked by PYR-41 (data not shown), PYR-41 could not affect the Atg14L puncta formation induced by p62 and Dvl2 aggregates (Fig. 6*H*). These data further demonstrate that ubiquitination is not essential for the autophagy initiation induced by protein aggregates.

DISCUSSION

Dvl proteins are key mediators of canonical and noncanonical Wnt signaling. The activity and stability of Dvl proteins are tightly controlled (17, 18, 36–38). We have reported that pVHL

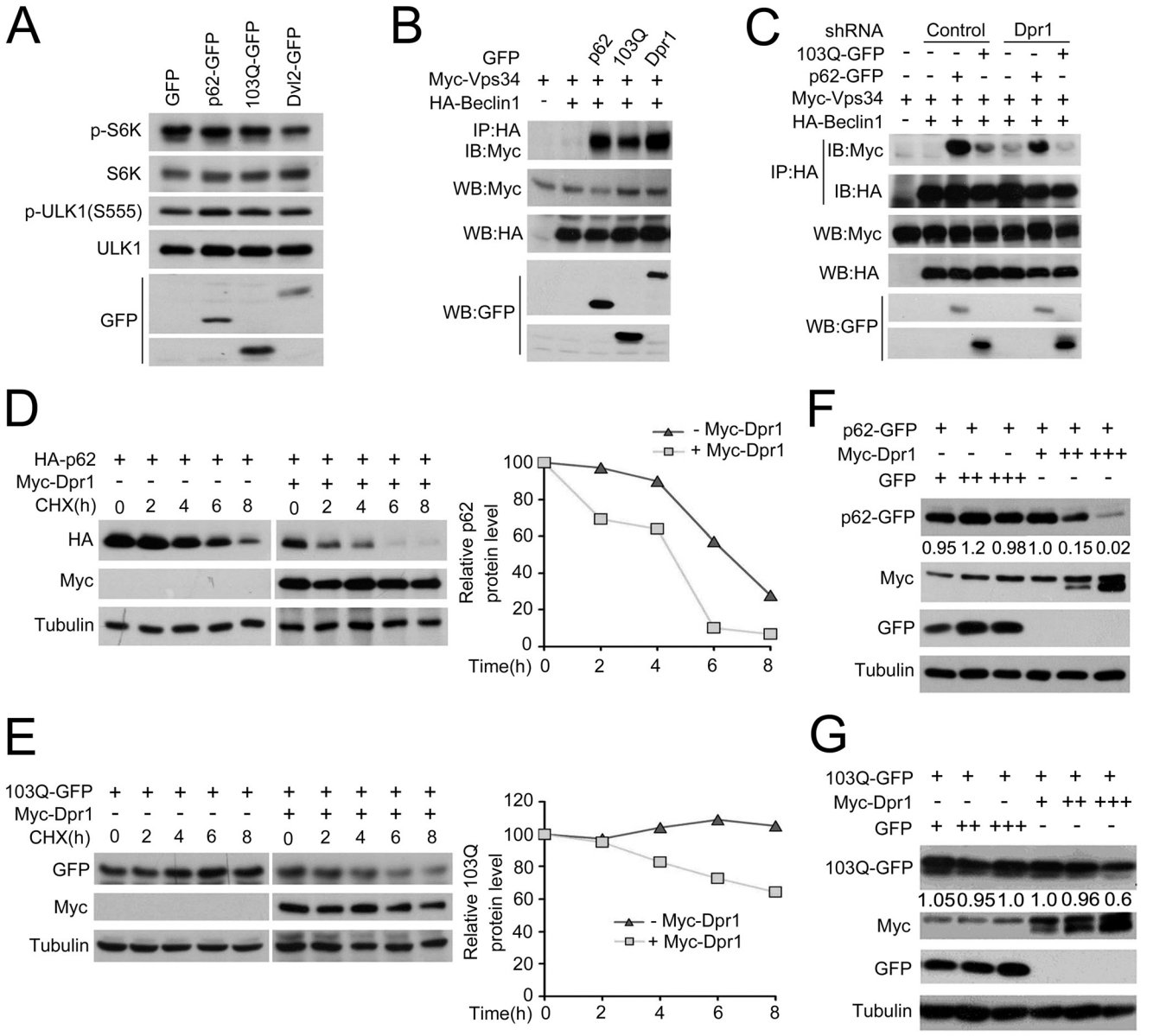

FIGURE 5. **Protein aggregate-enhanced Beclin1-Vps34 interaction depends on Dpr1.** *A,* aggregated proteins had no effect on AMP-activated protein kinase and mammalian target of rapamycin activity. HEK293T cells were transfected with the indicated plasmids and harvested for immunoblotting after 36 h. *B,* enhanced Vps34-Beclin1 interaction by ectopic expression of p62 or Htt103Q in HEK293T cells. *C,* induced Vps34-Beclin1 interaction by aggregates was reduced by *Dpr1* depletion in HEK293T cells. *D* and *E,* Dpr1 accelerated the degradation of p62-GFP (*D*) and Htt103Q-GFP (*E*) in HEK293T cells. The cells transfected with the indicated plasmids were treated with the translation inhibitor cycloheximide (*CHX*) (10 μM) for various times before harvested for immunoblotting. The relative band intensity of p62 and Htt103Q was quantified and is shown at *right*. *F* and *G,* Dpr1 enhanced the degradation of p62-GFP (*F*) and Htt103Q-GFP (*G*) in a dose-dependent manner in HEK293T cells. HEK293T cells were transfected with indicated plasmids and harvested after 36 h. The band intensity of indicated proteins was quantified and normalized against to tubulin. *IP*, immunoprecipitation; *WB*, Western blot.

mediates Dvl2 ubiquitination, which is associated with Dvl2 aggregation and enhances its degradation via autophagy (15). In this study, we found that Dpr1 promoted the interaction between Dvl2 and pVHL and therefore accelerated the autophagy-mediated degradation of Dvl2. As Dpr1 can also facilitate autophagy initiation (20), it seems that Dpr1 promotes the autophagy-mediated degradation of Dvl2 in two independent ways: on the one hand, Dpr1 enhances the autophagy initiation process by activating the Vps34-Beclin1-Atg14L complex; on the other hand, Dpr1 acts as an adaptor to increase the ubiquitination of Dvl2 mediated by the E3 ligase pVHL. Both Dpr1 functions lead to the accelerated degradation of Dvl2 via autophagy.

Although it has been known for a long time that aggregated proteins can be degraded in lysosomes through autophagy (8, 39–41), it is unclear whether aggregated proteins could stimulate autophagy and enhance their degradation in a feedback manner. Here, we have demonstrated that the aggregation-prone proteins such as Dvl2, p62, and Htt103Q can increase the Vps34-Beclin1 interaction and Atg14L puncta formation, therefore facilitating the initiation of autophagy. We have also demonstrated that Dpr1 is critical in this process as p62-induced Atg14L puncta formation was much reduced in *Dpr1* knock-out cells.

How the protein aggregates activate the autophagy initiating machinery is still an open question. Although wild-type Dvl2

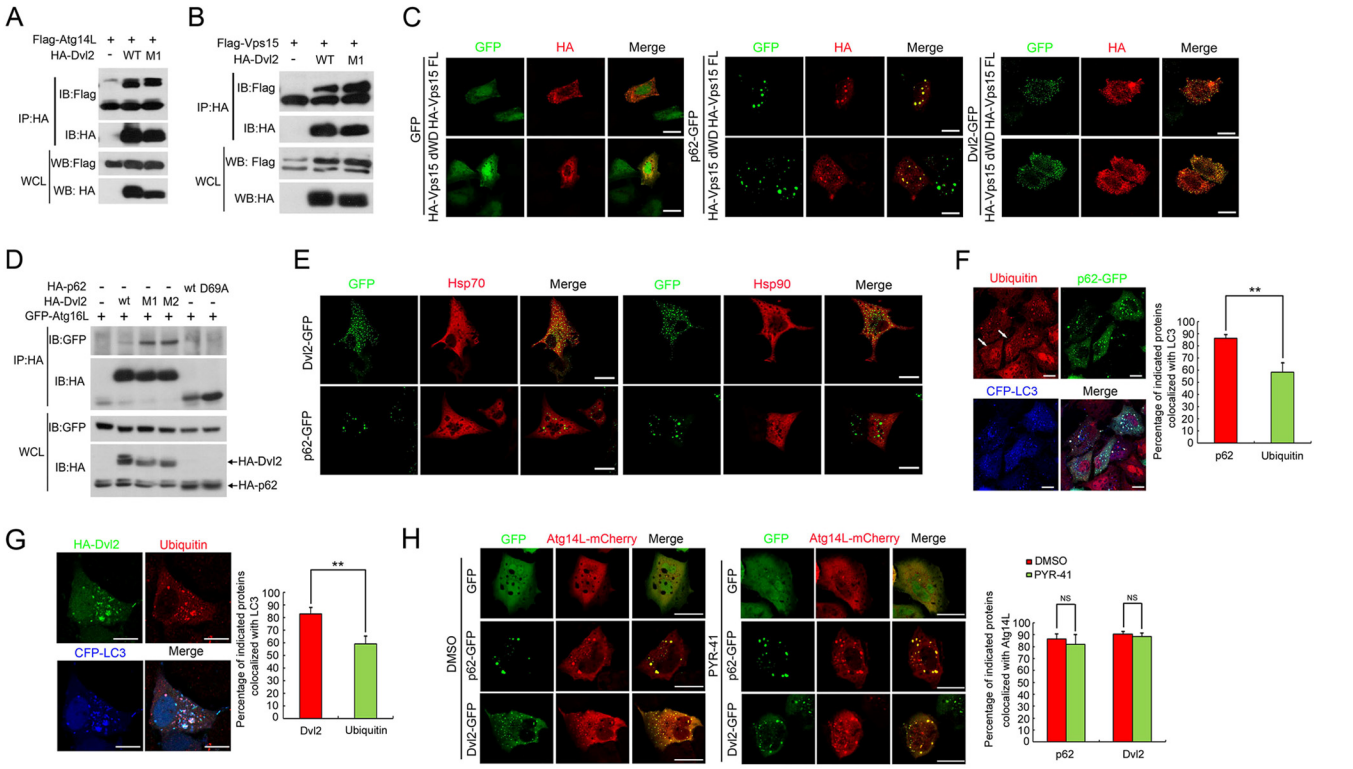

FIGURE 6. **Ubiquitination is not essential for the aggregate-induced autophagy initiation.** *A* and *B*, Atg14L (*A*) and Vps15 (*B*) bind equally to the wild-type Dvl2 and its M1 mutant. HEK293T cells transfected with the indicated constructs were harvested for immunoprecipitation (*IP*) by anti-HA antibody, following by anti-FLAG immunoblotting (*IB*). *WCL*, whole cell lysate. *C*, WD40 domain of Vps15 was not required for aggregate-induced Vps15 puncta formation. NRK cells transfected with the indicated plasmids were fixed with 4% paraformaldehyde for immunofluorescence. *Scale bars*, 10 μm. *Vps15 FL*, full length of Vps15; *Vps15 dWD*, WD40 domain deletion of Vps15. *D*, interaction of Atg16L with Dvl2, p62, and their aggregation-deficient mutants. *E*, Hsp70 and Hsp90 did not form puncta upon Dvl2 or p62 overexpression. *Scale bars*, 10 μm. *F* and *G*, endogenous ubiquitin was not always colocalized with the p62 and LC3 double-positive puncta (*F*) or Dvl2 and LC3 double-positive puncta (*G*). NRK cells transfected with the indicated plasmids were fixed with 4% paraformaldehyde for immunofluorescence. The percentage of LC3-positive dots colocalized with p62 or ubiquitin (*F*) or colocalized with Dvl2 or ubiquitin (*G*) was calculated ($n = 3$). *Scale bars*, 10 μm. *Arrows* indicate the cells lacking the p62-LC3-ubiquitin colocalization. Data are represented as mean ± S.D. *H*, PYR-41 did not block the Atg14L puncta formation induced by Dvl2 and p62. NRK cells transfected with indicated plasmids were treated with 50 μM PYR-41 for 24 h and fixed for immunofluorescence. The percentage of Atg14L-positive dots colocalized with p62 or Dvl2 was calculated ($n = 3$). *Scale bars*, 10 μm. NS means no significance. Data were represented as mean ± S.D. **, $p < 0.01$.

interacts with LC3 stronger than its aggregation-deficient M1 and M2 mutants (15), none of the autophagy initiation machinery components, Vps15, Atg14L, and Atg16L, showed a better binding ability with wild-type Dvl2 than with the M1 mutant, indicating that these machinery components may not specifically recognize the aggregated substrates. This notion was supported by the data that Atg16L did not apparently interact with either wild-type p62 or its aggregation-deficient D69A mutant.

Ubiquitination plays an important role in the degradation of protein aggregates via autophagy (33, 34). Ubiquitin has been shown to be critical for the recruitment of the autophagic machinery to endosomes to mediate pathogen clearance during *Salmonella* infection (30). However, aggregate-induced autophagy may not necessarily require ubiquitination as some of the LC3 puncta induced by aggregates were stained negatively for endogenous ubiquitin. In addition, the inhibition of ubiquitin-conjugated E1 activity by PYR-41 did not block the aggregate-induced Atg14L puncta formation. However, our immunofluorescence analysis revealed that many p62 and Dvl2 aggregate-induced LC3 puncta were positively stained with ubiquitin. Therefore, we could not exclude the possible function of ubiquitination in selective aggrephagy. Other proteins could bridge the aggregates directly to the autophagy machinery. For instance, optineurin has been shown to interact with protein aggregates associated with neurodegenerative diseases via its C-terminal coiled-coil domain (42). This interaction is ubiquitin-independent. As optineurin contains an LC3-interacting motif, it promotes aggrephagy by recruiting aggregates to autophagosomes (42). It will be interesting to test whether optineurin can mediate aggregate-induced autophagy initiation by promoting Beclin1-Vps34 complex formation. Nonetheless, this study provides a new for Dpr1 in aggrephagy.

Acknowledgments—We thank Drs. Li Yu (Tsinghua University), Hong Zhang (Institute of Biophysics, Chinese Academy of Sciences), Zhijie Chang (Tsinghua University), and Honggang Wang (Pennsylvania State University College of Medicine) for plasmids.

REFERENCES

1. Shibutani, S. T., and Yoshimori, T. (2014) A current perspective of autophagosome biogenesis. *Cell Res.* **24,** 58–68
2. Hurley, J. H., and Schulman, B. A. (2014) Atomistic autophagy: the structures of cellular self-digestion. *Cell* **157,** 300–311
3. Feng, Y., He, D., Yao, Z., and Klionsky, D. J. (2014) The machinery of macroautophagy. *Cell Res.* **24,** 24–41
4. Mizushima, N., Yoshimori, T., and Ohsumi, Y. (2011) The role of Atg

proteins in autophagosome formation. *Annu. Rev. Cell Dev. Biol.* **27,** 107–132
5. Mizushima, N., and Komatsu, M. (2011) Autophagy: renovation of cells and tissues. *Cell* **147,** 728–741
6. Dall'Armi, C., Devereaux, K. A., and Di Paolo, G. (2013) The role of lipids in the control of autophagy. *Curr. Biol.* **23,** R33–R45
7. Kraft, C., and Martens, S. (2012) Mechanisms and regulation of autophagosome formation. *Curr. Opin. Cell Biol.* **24,** 496–501
8. Lamark, T., and Johansen, T. (2012) Aggrephagy: selective disposal of protein aggregates by macroautophagy. *Int. J. Cell Biol.* 2012, 736905
9. Lamark, T., Kirkin, V., Dikic, I., and Johansen, T. (2009) NBR1 and p62 as cargo receptors for selective autophagy of ubiquitinated targets. *Cell Cycle* **8,** 1986–1990
10. Pankiv, S., Clausen, T. H., Lamark, T., Brech, A., Bruun, J. A., Outzen, H., Øvervatn, A., Bjørkøy, G., and Johansen, T. (2007) p62/SQSTM1 binds directly to Atg8/LC3 to facilitate degradation of ubiquitinated protein aggregates by autophagy. *J. Biol. Chem.* **282,** 24131–24145
11. Filimonenko, M., Isakson, P., Finley, K. D., Anderson, M., Jeong, H., Melia, T. J., Bartlett, B. J., Myers, K. M., Birkeland, H. C., Lamark, T., Krainc, D., Brech, A., Stenmark, H., Simonsen, A., and Yamamoto, A. (2010) The selective macroautophagic degradation of aggregated proteins requires the PI3P-binding protein Alfy. *Mol. Cell* **38,** 265–279
12. Wong, E., Bejarano, E., Rakshit, M., Lee, K., Hanson, H. H., Zaarur, N., Phillips, G. R., Sherman, M. Y., and Cuervo, A. M. (2012) Molecular determinants of selective clearance of protein inclusions by autophagy. *Nat. Commun.* **3,** 1240
13. Anastas, J. N., and Moon, R. T. (2013) WNT signalling pathways as therapeutic targets in cancer. *Nat. Rev. Cancer* **13,** 11–26
14. Clevers, H., and Nusse, R. (2012) Wnt/β-catenin signaling and disease. *Cell* **149,** 1192–1205
15. Gao, C., Cao, W., Bao, L., Zuo, W., Xie, G., Cai, T., Fu, W., Zhang, J., Wu, W., Zhang, X., and Chen, Y. G. (2010) Autophagy negatively regulates Wnt signalling by promoting Dishevelled degradation. *Nat. Cell Biol.* **12,** 781–790
16. Cheyette, B. N., Waxman, J. S., Miller, J. R., Takemaru, K., Sheldahl, L. C., Khlebtsova, N., Fox, E. P., Earnest, T., and Moon, R. T. (2002) Dapper, a Dishevelled-associated antagonist of β-catenin and JNK signaling, is required for notochord formation. *Dev. Cell* **2,** 449–461
17. Chen, H., Liu, L., Ma, B., Ma, T. M., Hou, J. J., Xie, G. M., Wu, W., Yang, F. Q., and Chen, Y. G. (2011) Protein kinase A-mediated 14–3-3 association impedes human Dapper1 to promote dishevelled degradation. *J. Biol. Chem.* **286,** 14870–14880
18. Wen, J., Chiang, Y. J., Gao, C., Xue, H., Xu, J., Ning, Y., Hodes, R. J., Gao, X., and Chen, Y. G. (2010) Loss of Dact1 disrupts planar cell polarity signaling by altering dishevelled activity and leads to posterior malformation in mice. *J. Biol. Chem.* **285,** 11023–11030
19. Zhang, L., Gao, X., Wen, J., Ning, Y., and Chen, Y. G. (2006) Dapper 1 antagonizes Wnt signaling by promoting dishevelled degradation. *J. Biol. Chem.* **281,** 8607–8612
20. Ma, B., Cao, W., Li, W., Gao, C., Qi, Z., Zhao, Y., Du, J., Xue, H., Peng, J., Wen, J., Chen, H., Ning, Y., Huang, L., Zhang, H., Gao, X., *et al.* (2014) Dapper1 promotes autophagy by enhancing the Beclin1-Vps34-Atg14L complex formation. *Cell Res.* **24,** 912–924
21. Klionsky, D. J., Abdalla, F. C., Abeliovich, H., Abraham, R. T., Acevedo-Arozena, A., Adeli, K., Agholme, L., Agnello, M., Agostinis, P., Aguirre-Ghiso, J. A., Ahn, H. J., Ait-Mohamed, O., Ait-Si-Ali, S., Akematsu, T., Akira, S., *et al.* (2012) Guidelines for the use and interpretation of assays for monitoring autophagy. *Autophagy* **8,** 445–544
22. Mizushima, N., Yoshimori, T., and Levine, B. (2010) Methods in mammalian autophagy research. *Cell* **140,** 313–326
23. Kaelin, W. G. (2005) The von Hippel-Lindau tumor suppressor protein: roles in cancer and oxygen sensing. *Cold Spring Harb. Symp. Quant. Biol.* **70,** 159–166
24. Schwarz-Romond, T., Fiedler, M., Shibata, N., Butler, P. J., Kikuchi, A., Higuchi, Y., and Bienz, M. (2007) The DIX domain of Dishevelled confers Wnt signaling by dynamic polymerization. *Nat. Struct. Mol. Biol.* **14,** 484–492
25. Schwarz-Romond, T., Merrifield, C., Nichols, B. J., and Bienz, M. (2005) The Wnt signalling effector Dishevelled forms dynamic protein assemblies rather than stable associations with cytoplasmic vesicles. *J. Cell Sci.* **118,** 5269–5277
26. Bjørkøy, G., Lamark, T., Brech, A., Outzen, H., Perander, M., Overvatn, A., Stenmark, H., and Johansen, T. (2005) p62/SQSTM1 forms protein aggregates degraded by autophagy and has a protective effect on huntingtin-induced cell death. *J. Cell Biol.* **171,** 603–614
27. Yamamoto, A., Cremona, M. L., and Rothman, J. E. (2006) Autophagy-mediated clearance of huntingtin aggregates triggered by the insulin-signaling pathway. *J. Cell Biol.* **172,** 719–731
28. Itakura, E., and Mizushima, N. (2011) p62 targeting to the autophagosome formation site requires self-oligomerization but not LC3 binding. *J. Cell Biol.* **192,** 17–27
29. Pashkova, N., Gakhar, L., Winistorfer, S. C., Yu, L., Ramaswamy, S., and Piper, R. C. (2010) WD40 repeat propellers define a ubiquitin-binding domain that regulates turnover of F box proteins. *Mol. Cell* **40,** 433–443
30. Fujita, N., Morita, E., Itoh, T., Tanaka, A., Nakaoka, M., Osada, Y., Umemoto, T., Saitoh, T., Nakatogawa, H., Kobayashi, S., Haraguchi, T., Guan, J. L., Iwai, K., Tokunaga, F., Saito, K., *et al.* (2013) Recruitment of the autophagic machinery to endosomes during infection is mediated by ubiquitin. *J. Cell Biol.* **203,** 115–128
31. Chaari, A., Hoarau-Véchot, J., and Ladjimi, M. (2013) Applying chaperones to protein-misfolding disorders: molecular chaperones against α-synuclein in Parkinson's disease. *Int. J. Biol. Macromol.* **60,** 196–205
32. Yang, Y., Fiskus, W., Yong, B., Atadja, P., Takahashi, Y., Pandita, T. K., Wang, H. G., and Bhalla, K. N. (2013) Acetylated hsp70 and KAP1-mediated Vps34 SUMOylation is required for autophagosome creation in autophagy. *Proc. Natl. Acad. Sci. U.S.A.* **110,** 6841–6846
33. Kirkin, V., McEwan, D. G., Novak, I., and Dikic, I. (2009) A role for ubiquitin in selective autophagy. *Mol. Cell* **34,** 259–269
34. Rogov, V., Dötsch, V., Johansen, T., and Kirkin, V. (2014) Interactions between autophagy receptors and ubiquitin-like proteins form the molecular basis for selective autophagy. *Mol. Cell* **53,** 167–178
35. Yang, Y., Kitagaki, J., Dai, R. M., Tsai, Y. C., Lorick, K. L., Ludwig, R. L., Pierre, S. A., Jensen, J. P., Davydov, I. V., Oberoi, P., Li, C. C., Kenten, J. H., Beutler, J. A., Vousden, K. H., and Weissman, A. M. (2007) Inhibitors of ubiquitin-activating enzyme (E1), a new class of potential cancer therapeutics. *Cancer Res.* **67,** 9472–9481
36. Gao, C., and Chen, Y. G. (2010) Dishevelled: The hub of Wnt signaling. *Cell. Signal.* **22,** 717–727
37. Ding, Y., Zhang, Y., Xu, C., Tao, Q. H., and Chen, Y. G. (2013) HECT domain-containing E3 ubiquitin ligase NEDD4L negatively regulates Wnt signaling by targeting dishevelled for proteasomal degradation. *J. Biol. Chem.* **288,** 8289–8298
38. Suriben, R., Kivimäe, S., Fisher, D. A., Moon, R. T., and Cheyette, B. N. (2009) Posterior malformations in Dact1 mutant mice arise through misregulated Vangl2 at the primitive streak. *Nat. Genet.* **41,** 977–985
39. Jiang, P., and Mizushima, N. (2014) Autophagy and human diseases. *Cell Res.* **24,** 69–79
40. Svenning, S., and Johansen, T. (2013) Selective autophagy. *Essays Biochem.* **55,** 79–92
41. Rubinsztein, D. C., Mariño, G., and Kroemer, G. (2011) Autophagy and aging. *Cell* **146,** 682–695
42. Korac, J., Schaeffer, V., Kovacevic, I., Clement, A. M., Jungblut, B., Behl, C., Terzic, J., and Dikic, I. (2013) Ubiquitin-independent function of optineurin in autophagic clearance of protein aggregates. *J. Cell Sci.* **126,** 580–592